Figures

The Paranasal Air Sinuses of Predatory and Armored Dinosaurs (Archosauria: Theropoda and Ankylosauria) and Their Contribution to Cephalic Structure

LAWRENCE M. WITMER AND RYAN C. RIDGELY

citation:
Witmer, L. M., and R. C. Ridgely. 2008. The paranasal air sinuses of predatory and armored dinosaurs (Archosauria: Theropoda and Ankylosauria) and their contribution to cephalic architecture. Anatomical Record 291:1362–1388.

WitmerLab web page with downloads of movies and 3D PDFs:
http://www.oucom.ohiou.edu/dbms-witmer/DinoSinuses_main.htm

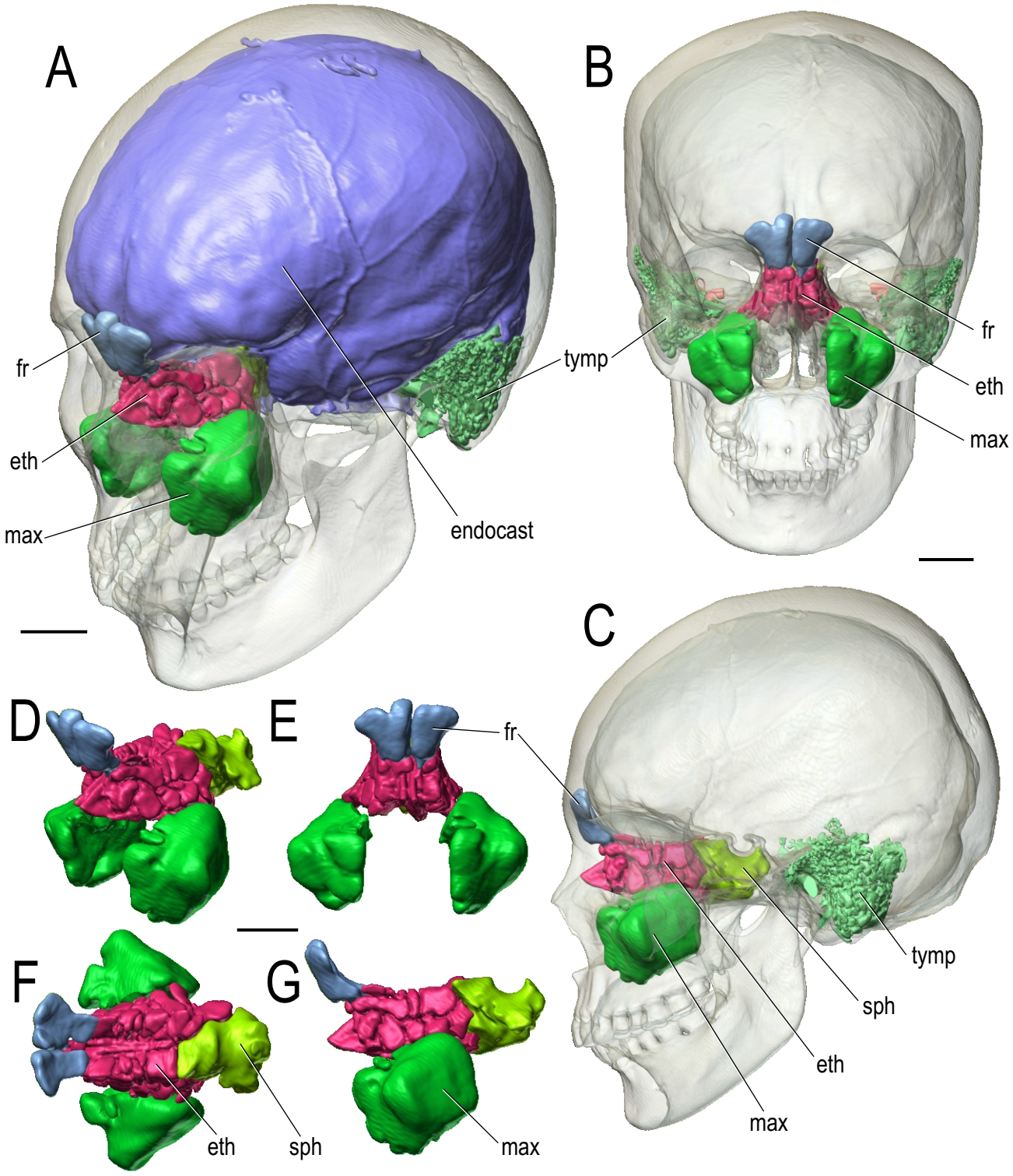

Fig. 1. Paranasal sinuses and other cephalic components of a human (*Homo sapiens*, OUVC 10503) based on CT scanning followed by segmentation and 3D visualization. Bone is rendered semitransparent. **A:** Left anterodorsolateral view. **B:** Anterior view. **C:** Left lateral view. **D–G:** isolated paranasal sinuses. **D:** Left anterodorsolateral view corresponding to **A**. **E:** Anterior view corresponding to **B**. **F:** Dorsal view. **G:** Left lateral view corresponding to **C**. The paratympanic sinuses and endosseous labyrinth are also visualized. Scale bars = 2 cm.

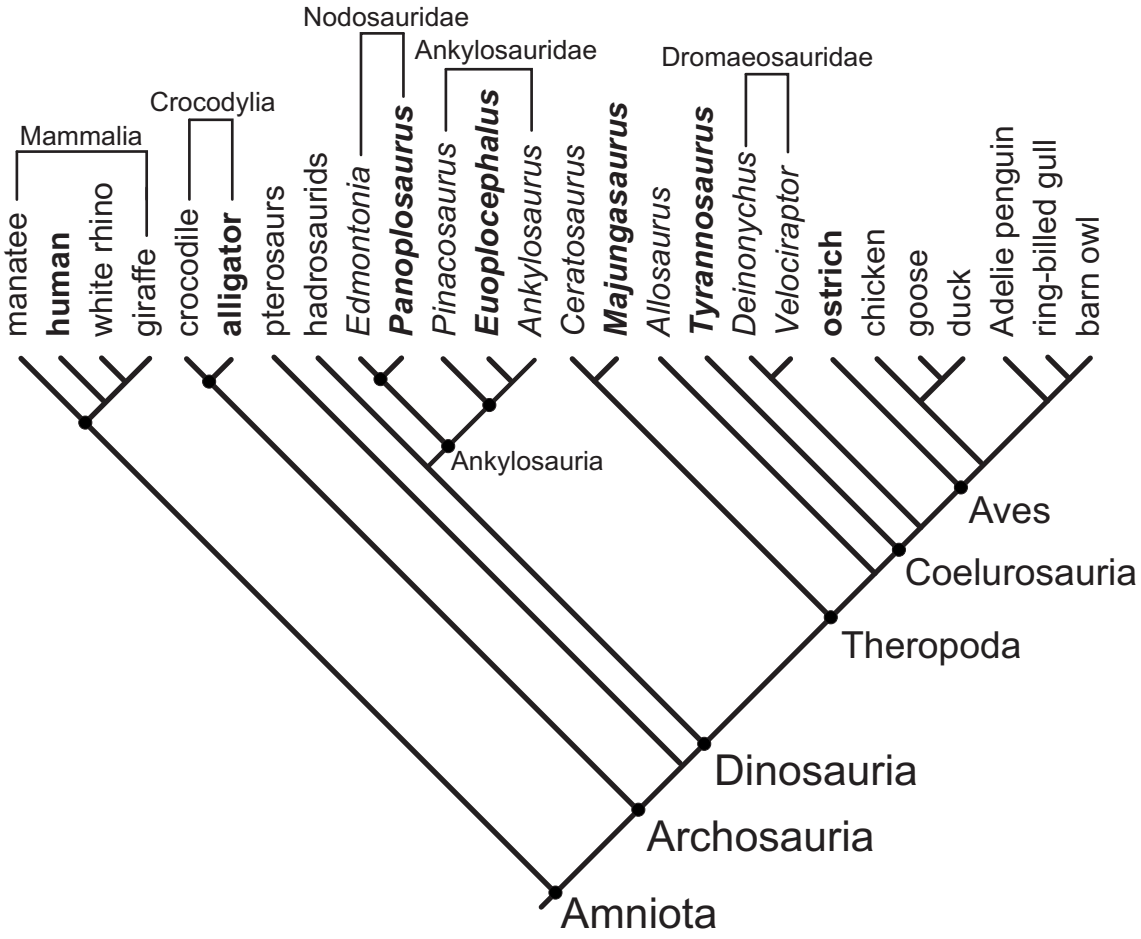

Fig. 2. Diagram of phylogenetic relationships of the taxa mentioned in the text. The focal taxa are indicated in boldface type. Topology derives from Hill et al. (2003), Holtz et al. (2004), Vickaryous et al. (2004), Bininda-Emonds et al. (2007), and Livezey and Zusi (2007).

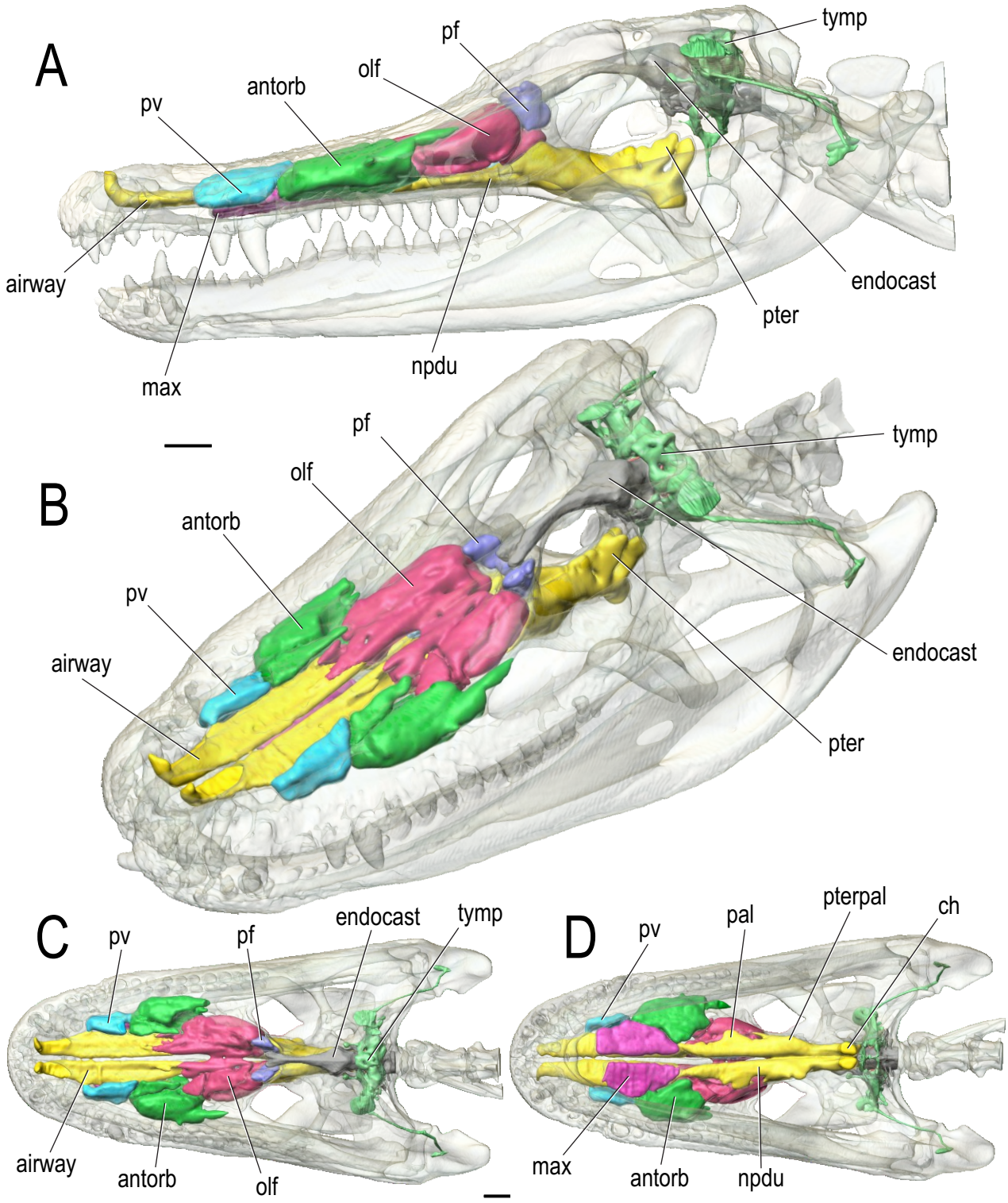

Fig. 3. Paranasal sinuses and other cephalic components of an American alligator (*Alligator mississippiensis*, OUVC 9761) based on CT scanning followed by segmentation and 3D visualization. Bone is rendered semitransparent. **A:** Left lateral view. **B:** Left rostrodorsolateral view. **C:** Dorsal view. **D:** Ventral view. Scale bars = 2 cm.

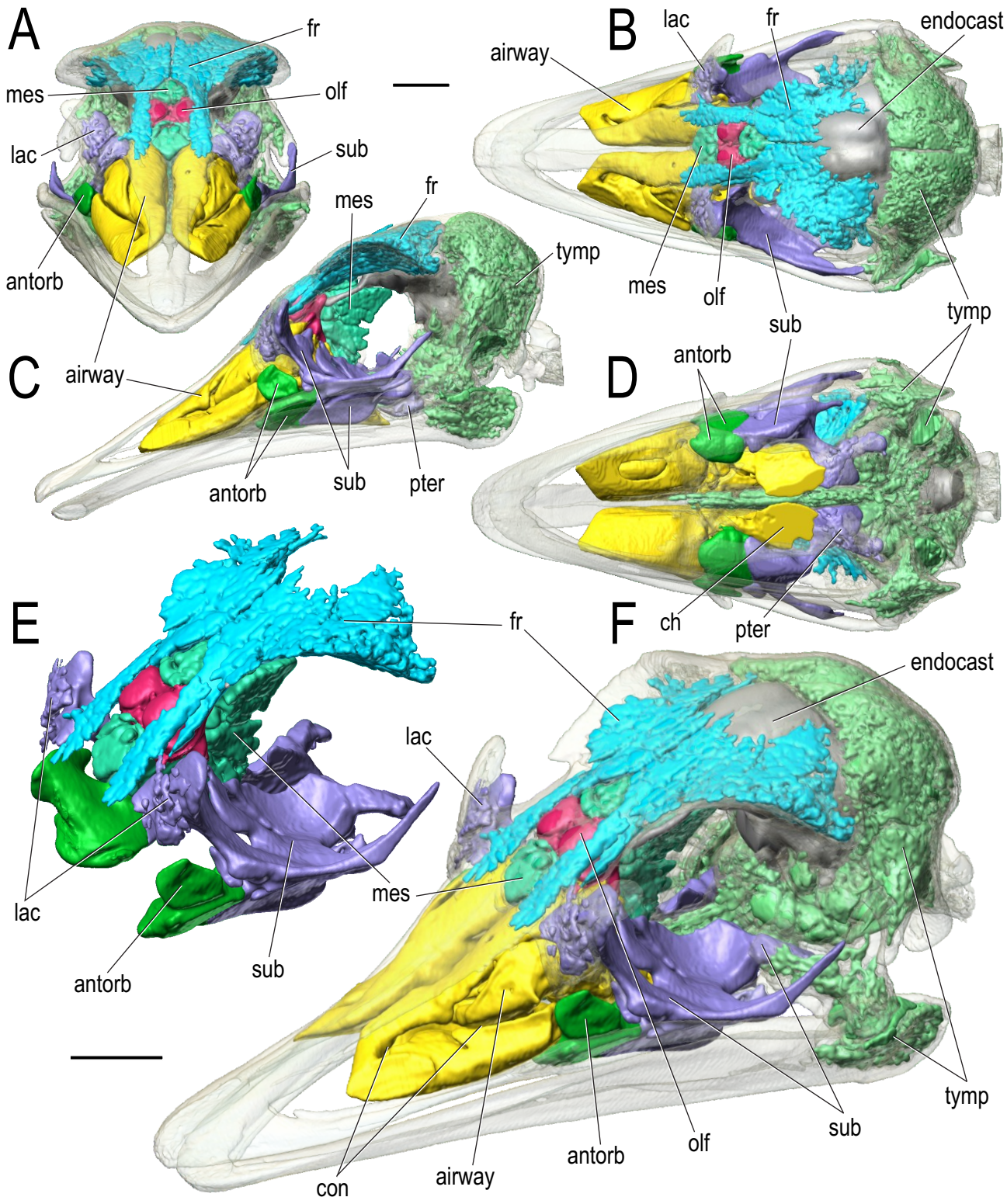

Fig. 4. Paranasal sinuses and other cephalic components of an ostrich (*Struthio camelus*, OUVC 10491) based on CT scanning followed by segmentation and 3D visualization. Bone is rendered semitransparent. **A:** Rostral view. **B:** Dorsal view. **C:** Left lateral view. **D:** Ventral view. **E:** Isolated paranasal sinuses in left rostrodorsolateral view. **F:** Left rostrodorsolateral view. Scale bars = 2 cm.

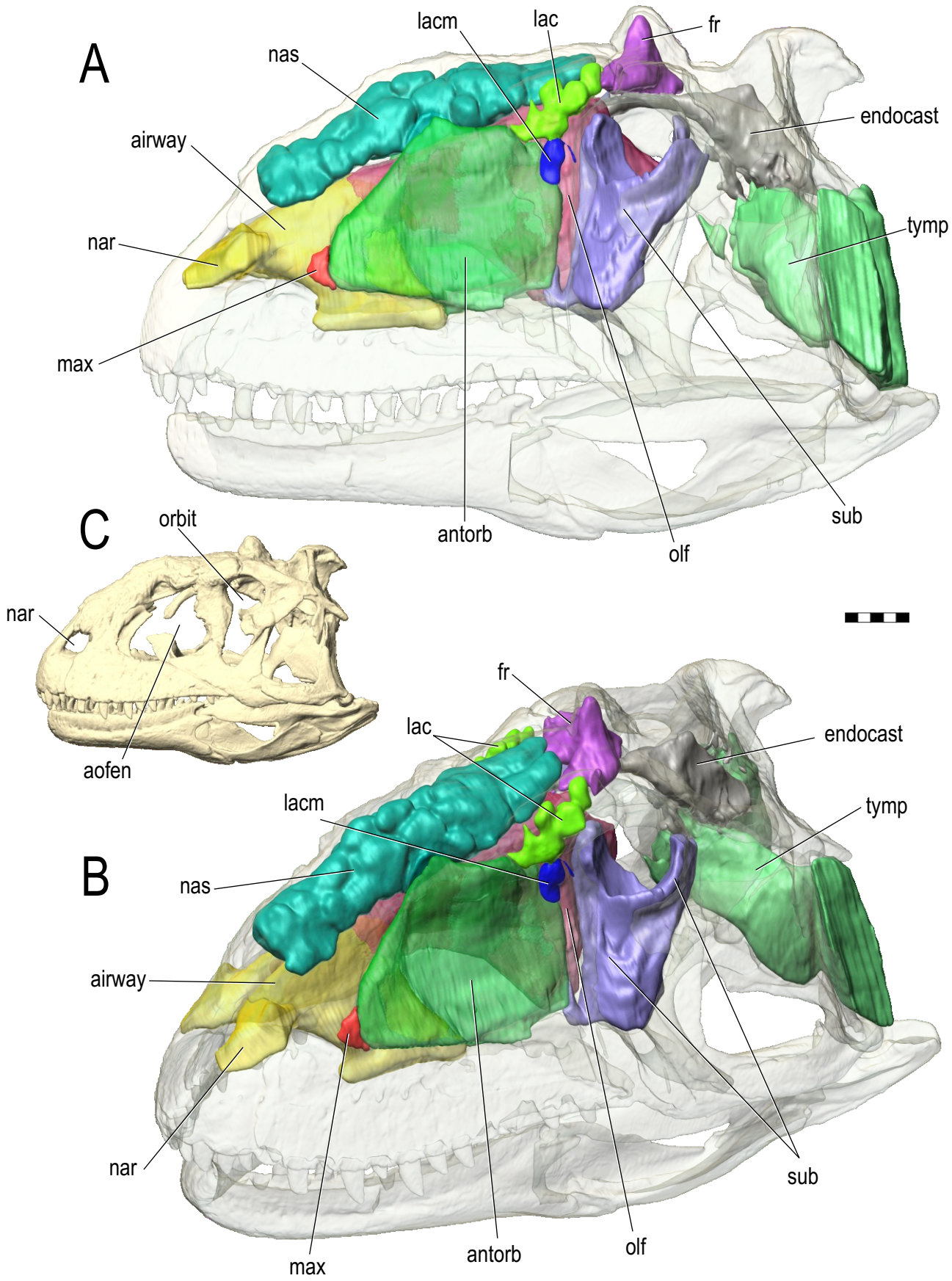

Fig. 5. Paranasal sinuses and other cephalic components of *Majungasaurus crenatissimus* (FMNH PR2100) based on CT scanning followed by segmentation and 3D visualization. Bone is rendered semitransparent (except in **C**), as is the nasal cavity (airway and olfactory region). **A:** Left lateral view. **B:** Left rostrodorsolateral view. **C:** Skull in left lateral view. **D:** Ventral view. **E:** Rostral view. **F:** Dorsal view. Scale bars = 5 cm.

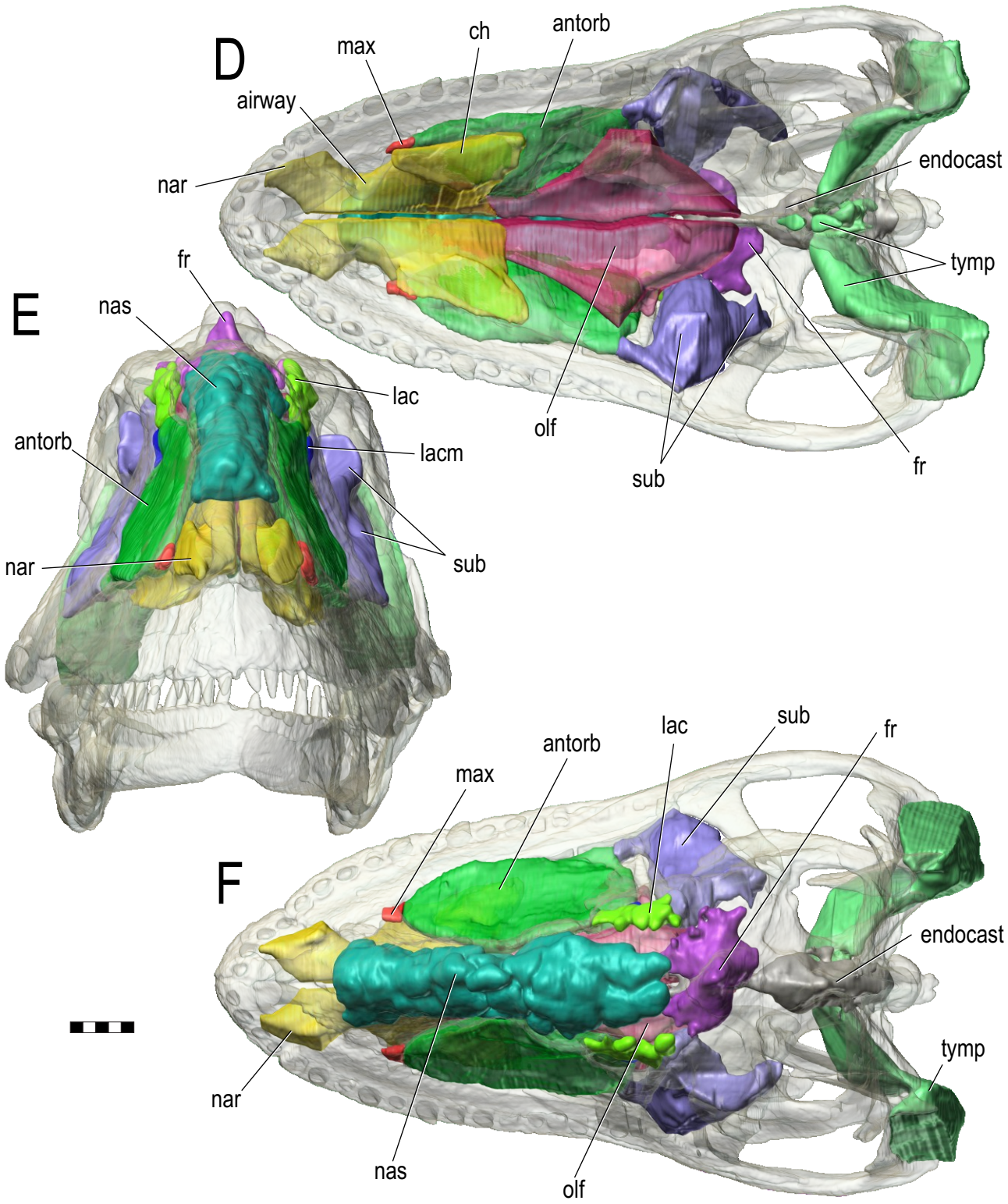
D
max
ch
antorb
airway
nar
endocast
tymp
fr
olf
sub
fr
E
nas
lac
antorb
lacm
nar
sub
F
max
antorb
lac
sub
fr
endocast
tymp
nar
nas
olf

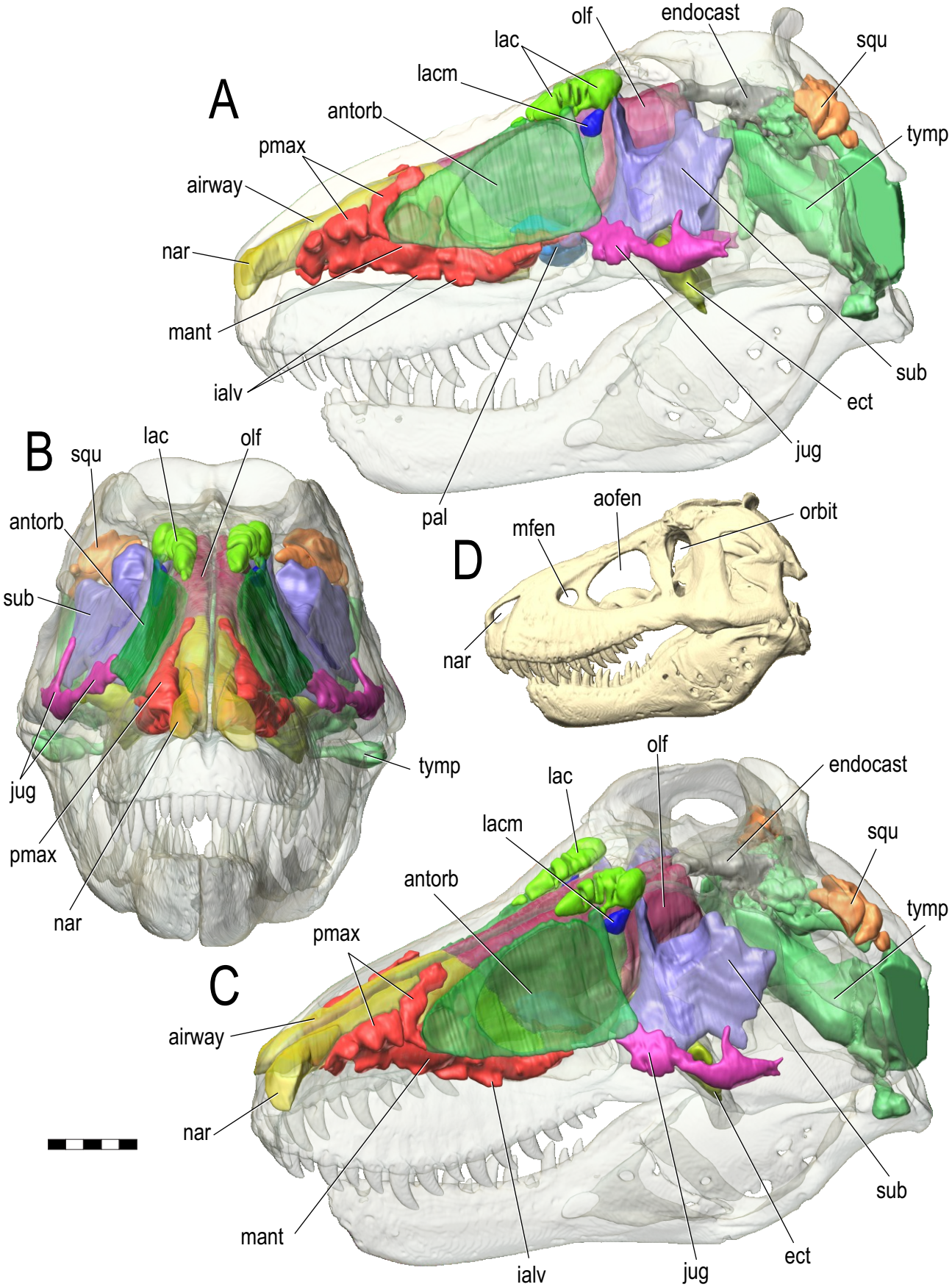

Fig. 6. Paranasal sinuses and other cephalic components of *Tyrannosaurus rex* (skull based on FMNH PR2081; soft-tissue components from several specimens, see text) based on CT scanning followed by segmentation and 3D visualization. Bone is rendered semitransparent (except in **D**), as is the nasal cavity (airway and olfactory region). **A:** Left lateral view. **B:** Rostral view. **C:** Left rostrodorsolateral view. **D:** Skull in left lateral view. **E:** Dorsal view. **F:** Ventral view. **G:** Right side of sagittally sectioned head in medial view. Scale bars = 20 cm.

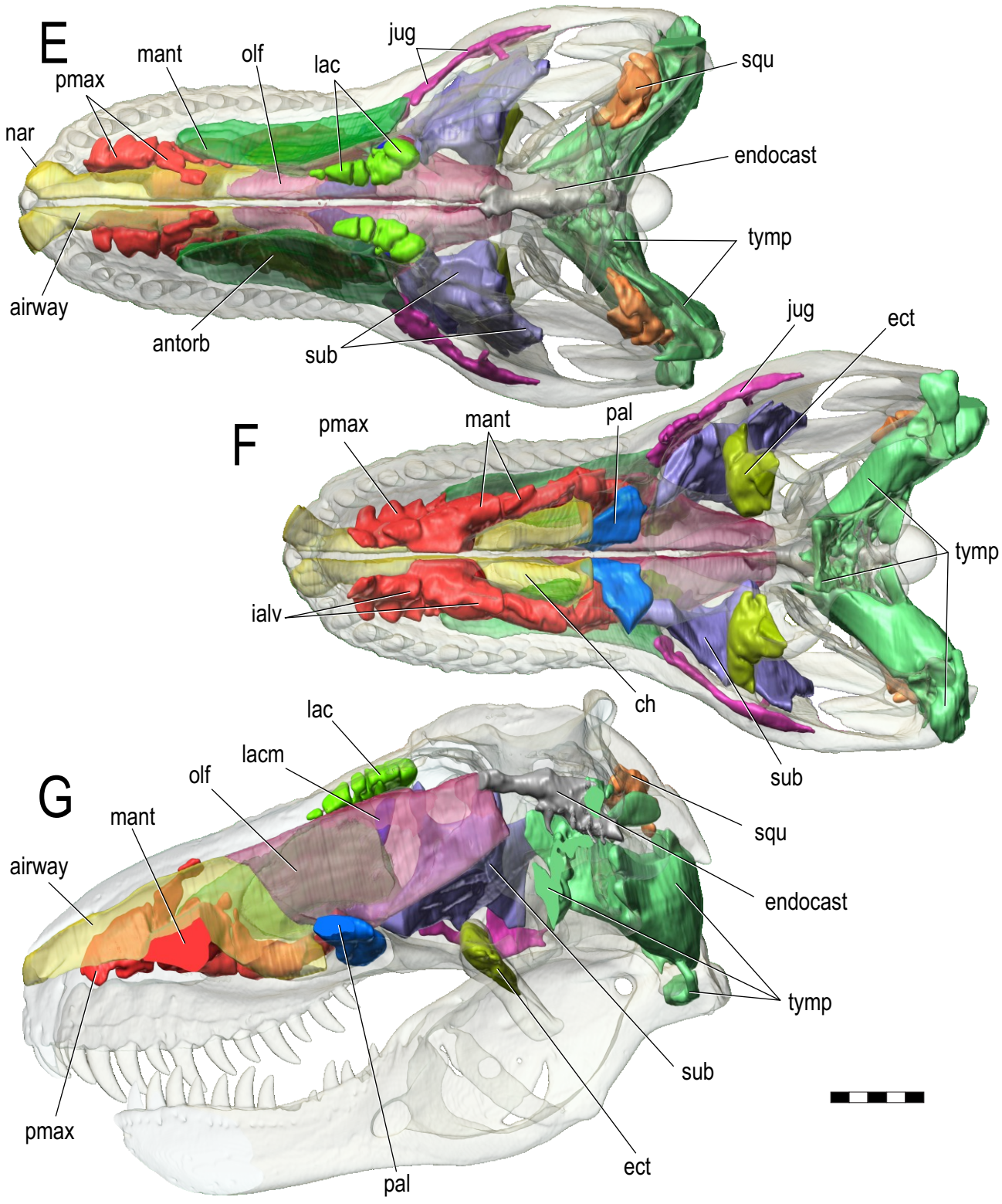
E
jug
mant
olf
lac
squ
pmax
nar
endocast
tymp
airway
antorb
sub
jug
ect
F
pmax
mant
pal
tymp
ialv
ch
sub
lac
lacm
olf
G
mant
squ
airway
endocast
tymp
sub
pmax
ect
pal

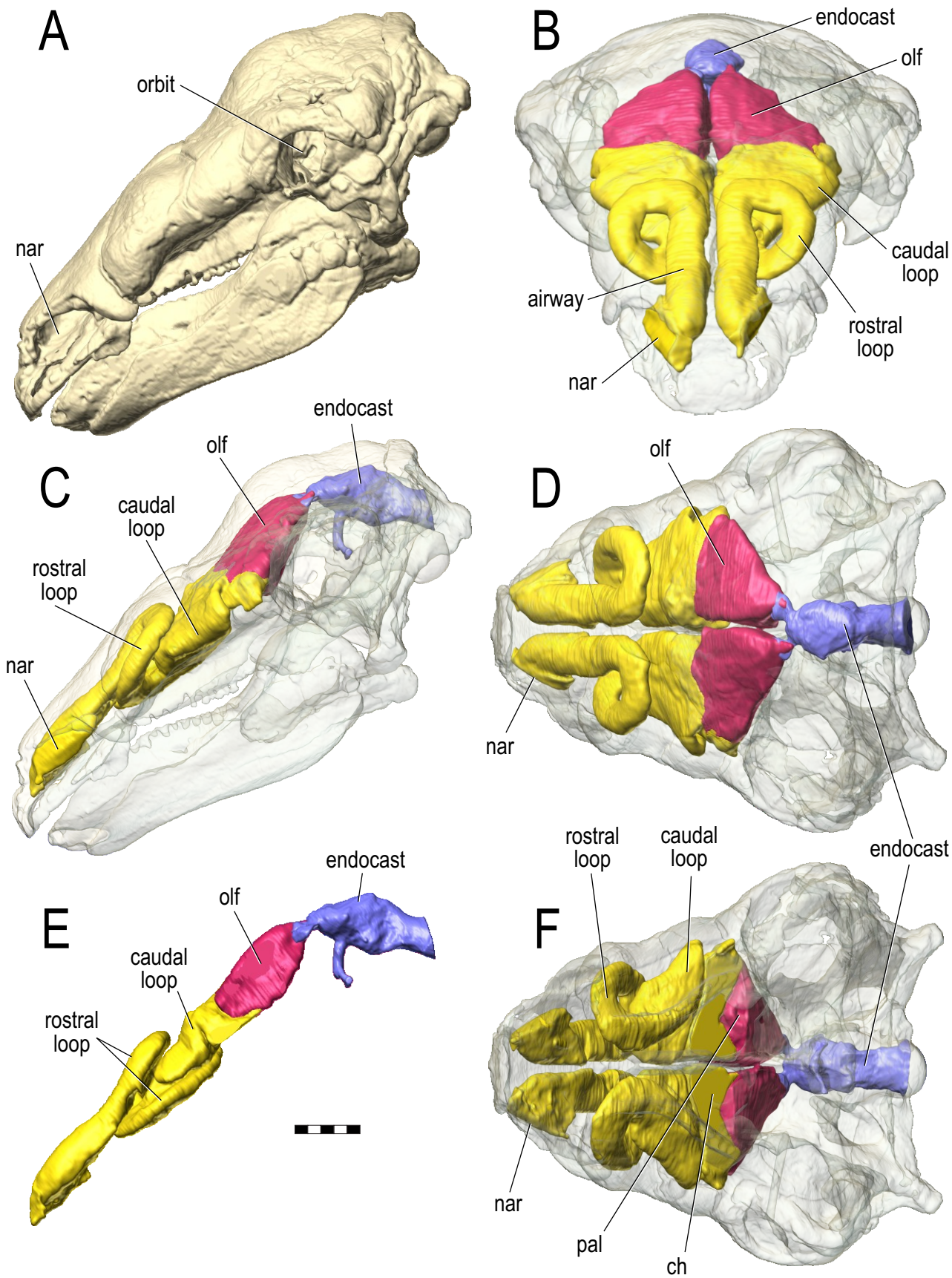

Fig. 7. Paranasal sinuses and other cephalic components of *Panoplosaurus mirus* (ROM 1215) based on CT scanning followed by segmentation and 3D visualization. Bone is rendered semitransparent (except in **A**). **A:** Skull in left lateral view. **B:** Rostral view. **C:** Left lateral view. **D:** Dorsal view. **E:** Right side of sagittally sectioned head in medial view with soft-tissue components isolated. **F:** Ventral view. **G:** Left rostrodorsolateral view. **H:** Isolated and semitransparent nasal cavity in left rostrodorsolateral view, revealing the course of the nasal airway (arrow). **B:** Same in left lateral view. Scale bars = 5 cm.

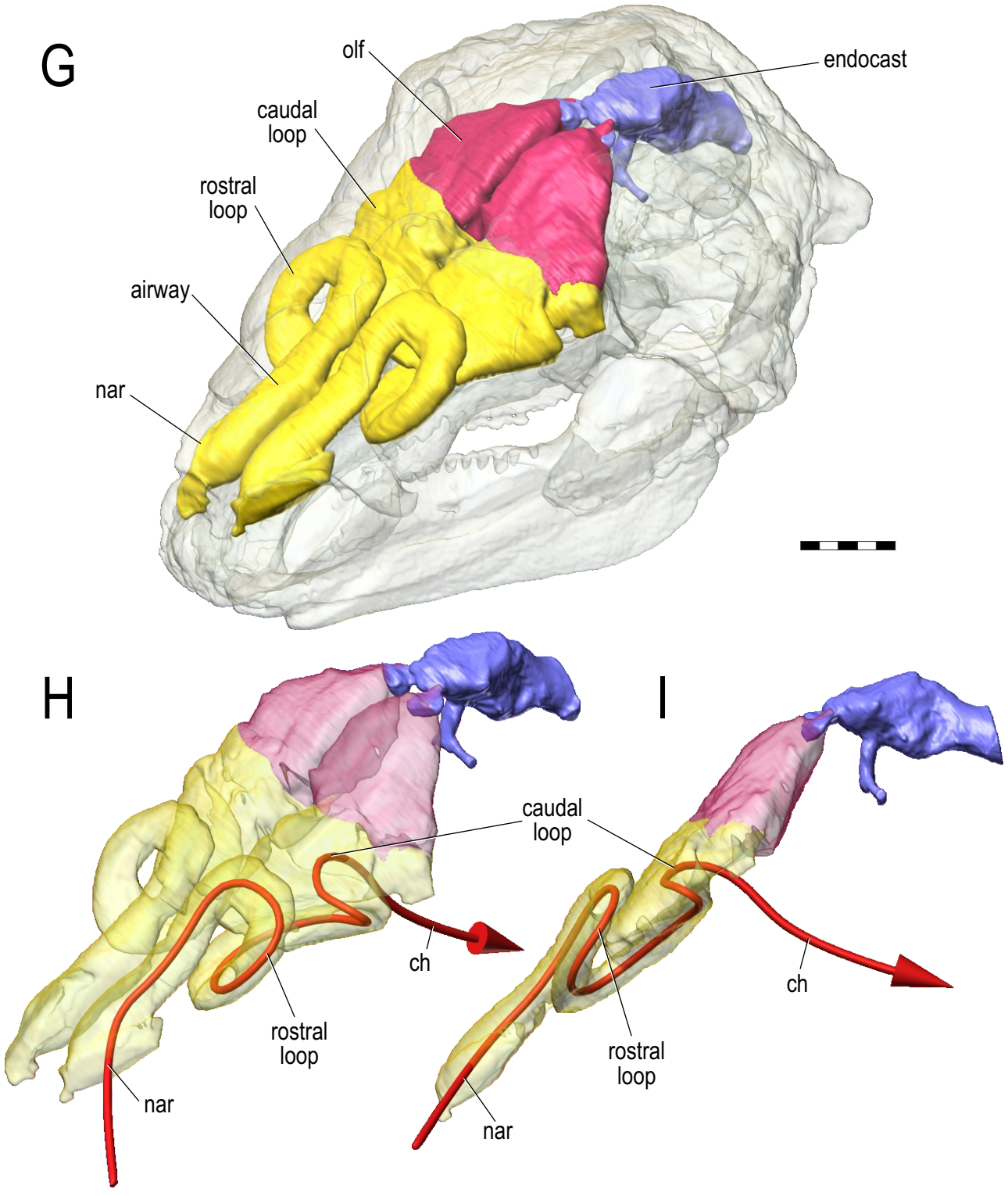
G
olf
endocast
caudal loop
rostral loop
airway
nar
H
caudal loop
ch
rostral loop
nar
I
caudal loop
ch
rostral loop
nar

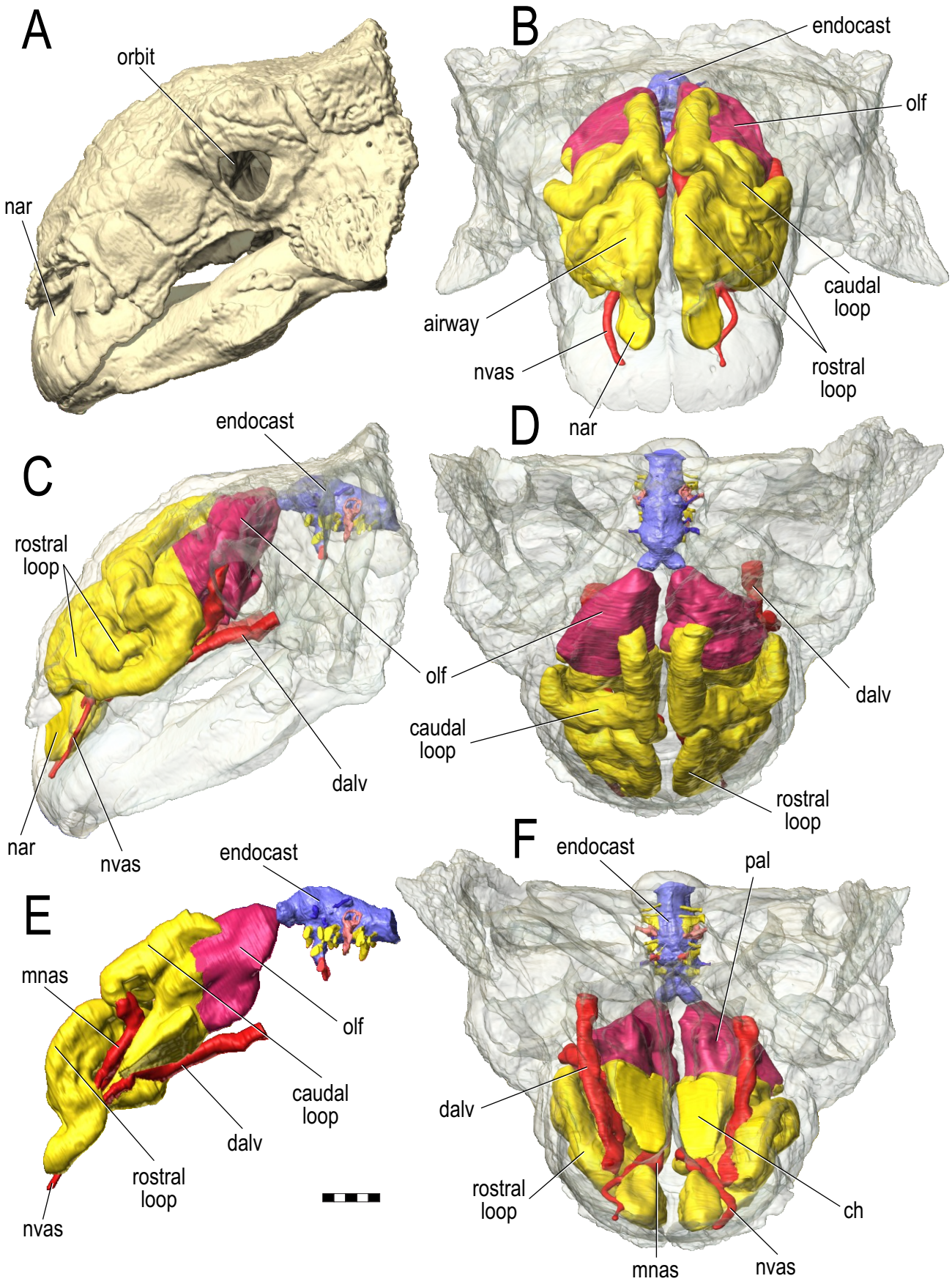

Fig. 8. Paranasal sinuses and other cephalic components of *Euoplocephalus tutus* (AMNH FR 5405) based on CT scanning followed by segmentation and 3D visualization. Bone is rendered semitransparent (except in **A**). **A:** Skull in left lateral view. **B:** Rostral view. **C:** Left lateral view. **D:** Dorsal view. **E:** Right side of sagittally sectioned head in medial view with soft-tissue components isolated. **F:** Ventral view. **G:** Left rostrodorsolateral view. **H:** Isolated and semitransparent nasal cavity in left rostrodorsolateral view, revealing the course of the nasal airway (arrow). **B:** Same in left lateral view. Scale bars = 5 cm.

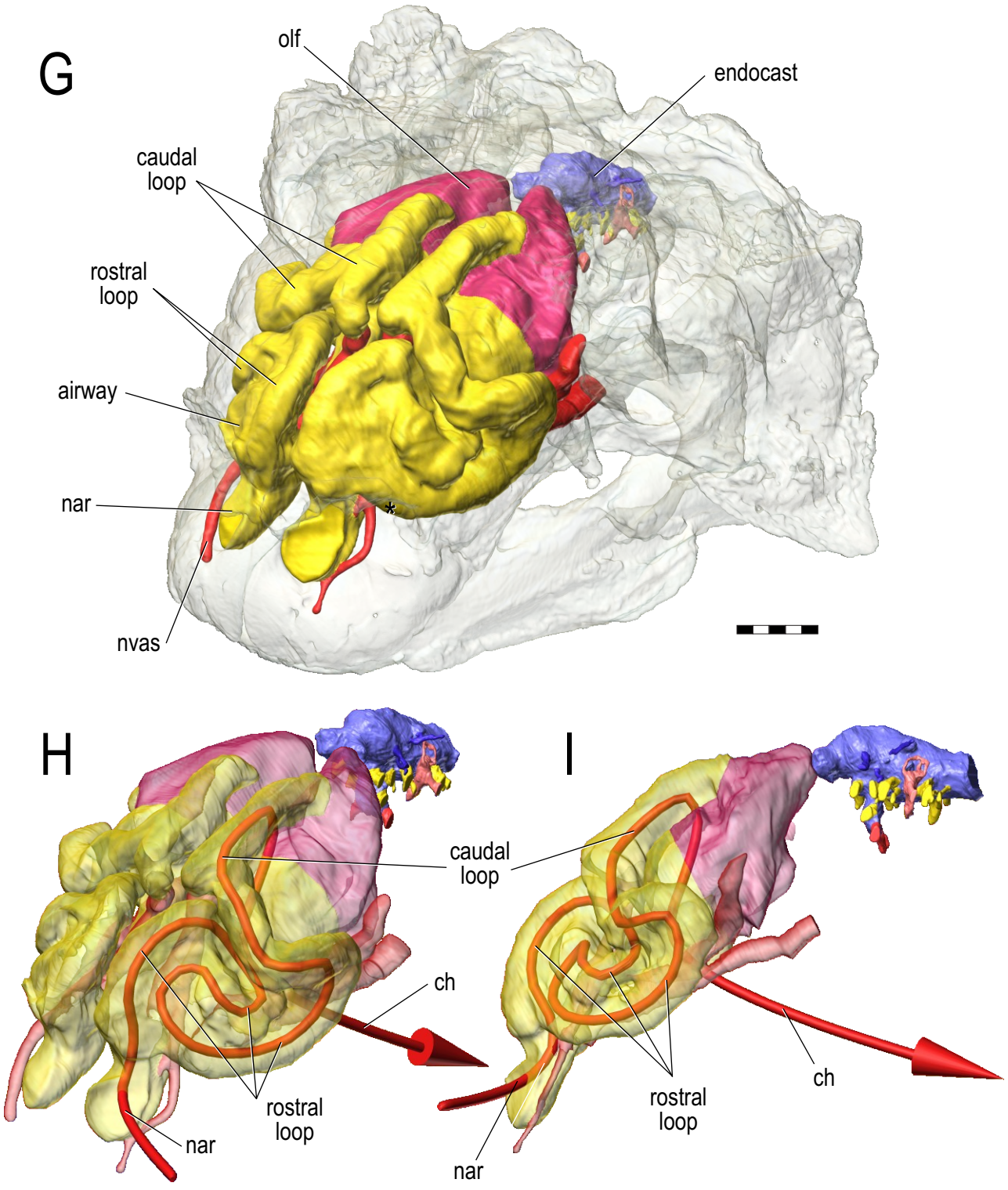
G
olf
endocast
caudal loop
rostral loop
airway
nar
nvas
H
caudal loop
ch
rostral loop
nar
I
caudal loop
ch
rostral loop
nar